



ATMOS/ATLAS 3 INFRARED PROFILE MEASUREMENTS OF TRACE GASES IN THE NOVEMBER 1994 TROPICAL AND SUBTROPICAL UPPER TROPOSPHERE

C. P. RINSLAND,^{†‡} M. R. GUNSON,[§] P.-H. WANG,^{||} R. F. ARDUINI,[¶]
 B. A. BAUM,[†] P. MINNIS,[†] A. GOLDMAN,^{††} M. C. ABRAMS,^{‡‡}
 R. ZANDER,^{§§} E. MAHIEU,^{§§} R. J. SALAWITCH,[§] H. A. MICHELSEN,^{||}
 F. W. IRION[§] and M. J. NEWCHURCH^{¶¶}

[†] Atmospheric Sciences Division, NASA Langley Research Center, Hampton, Virginia 23681, U.S.A.; [§] Jet Propulsion Laboratory, California Institute of Technology, 4800 Oak Grove Drive, Mail Stop 183-301, Pasadena, CA 91109, U.S.A.; ^{||} Science and Technology Corporation, 101 Research Drive, Hampton, VA 23666, U.S.A.; [¶] Science Applications International Corporation, 1 Enterprise Parkway, Suite 300, Hampton, VA 23666, U.S.A.; ^{††} Department of Physics, University of Denver, Denver, CO 80208, U.S.A.; ^{‡‡} ITT Defense and Electronics, 1919 W. Cook Road, P. O. Box 3700, Fort Wayne, IN 46801, U.S.A.; ^{§§} Institute of Astrophysics, University of Liège, Liège-Cointe, Belgium; ^{|||} Harvard University, Division of Applied Sciences, 12 Oxford Street, Cambridge, MA 02138, U.S.A. and ^{¶¶} Department of Atmospheric Science, University of Alabama in Huntsville, Huntsville, AL 35899, U.S.A.

(Received 12 May 1997; revised 8 January 1998)

Abstract—Vertical mixing ratio profiles of four relatively long-lived gases, HCN, C₂H₂, CO, and C₂H₆, have been retrieved from 0.01 cm⁻¹ resolution infrared solar occultation spectra recorded between latitudes of 5.3°N and 31.4°N. The observations were obtained by the Atmospheric Trace Molecule Spectroscopy (ATMOS) Fourier transform spectrometer during the Atmospheric Laboratory for Applications and Science (ATLAS) 3 shuttle flight, 3–12 November 1994. Elevated mixing ratios below the tropopause were measured for these gases during several of the occultations. The positive correlations obtained between the simultaneously measured mixing ratios suggest that the enhancements are likely the result of surface emissions, most likely biomass burning and/or urban industrial activities, followed by common injection via deep convective transport of the gases to the upper troposphere. The elevated levels of HCN may account for at least part of the “missing NO_y” in the upper troposphere. Comparisons of the observations with values measured during a recent aircraft campaign are presented. Published by Elsevier Science Ltd.

1. INTRODUCTION

Deep convection, driven in the tropics by the thermodynamical potential of water vapor evaporating from the Earth's warmest oceans,¹ provides the link between trace gases emitted near the surface and their occurrence in the upper troposphere. Ocean-derived and other natural chemicals and surface emissions due to pollution from biomass burning and urban/industrial regions are efficiently transported by tropical cloud currents to the upper troposphere with direct effects on ozone, sulfate aerosols, and trace gases.^{2–8} Wang et al³ simulated a deep convective storm observed during the Central Equatorial Pacific Experiment (CEPEX) and concluded that in addition to the vertical transport of boundary layer air with low ozone into the cloud, there may exist regions of high ozone, transported from the stratosphere to the upper part of the anvil. When convectively lifted, polluted airmasses from distant biomass fires can be converted from regions of net O₃ destruction to regions of net O₃ photochemical production⁹ with significant enhanced O₃ levels.¹⁰ Enhanced mixing ratios of CO and hydrocarbons originating from biomass burning were measured in the upper troposphere during the GTE/TRACE A (Global Tropospheric Experiment/Transport and Atmospheric Chemistry near the Equator-Atlantic) mission of September–October 1992.^{5–9}

[‡]To whom all correspondence should be addressed.

The purpose of this paper is to report vertical profile remote sensing measurements of HCN, CO, and the nonsoluble hydrocarbons C₂H₂ and C₂H₆ in the tropical and northern hemisphere subtropical upper troposphere. These four molecules have relatively long tropospheric lifetimes, and hence their concentrations may be influenced by multiple sources, over a large spatial region, each potentially with different emission fingerprints. In addition, dilution of enhanced mixing ratios with “background air” may lower the concentrations of these gases during transport.¹¹ The measurements were obtained in the solar occultation mode from low Earth orbit with the Atmospheric Trace Molecule Spectroscopy (ATMOS) Fourier transform spectrometer (FTS). We focus here on the analysis of these 4 molecules in spectra recorded with filters covering 625–1400 cm⁻¹ (filter 12) and 1550–3420 cm⁻¹ (filter 3). The accompanying paper reports a study of the same observations to quantify the extinction by cirrus ice clouds measured in some of the same spectra.¹² A brief description of the ATMOS/ATLAS 3 tropical and subtropical measurements is presented in Sec. 2. In Sec. 3, we describe the method used to analyze the spectra for trace gases, report the measured vertical profiles, and compare our results with tropical *in situ* observations obtained during a recent aircraft campaign. Finally, Sec. 4 gives a brief summary of the results.

2. ATMOS/ATLAS 3 TROPICAL AND SUBTROPICAL OBSERVATIONS

The ATMOS FTS was designed to record broad band 0.01 cm⁻¹ resolution mid-IR spectra from the shuttle during orbital surises and sunsets.^{13,14} Two-sided interferograms with a maximum optical path difference of 47 cm were measured at 2.2 s intervals during missions in 1985, 1992, 1993, and 1994. Typically, during a 4 min observations period, series of exoatmospheric (pure solar) and low Sun (atmospheric) spectra below a tangent altitude of ~150 km were recorded with one of a set of overlapping optical bandpass filters that limited the total spectral coverage to 625–4750 cm⁻¹. The results reported here were obtained during the Atmospheric Laboratory for Applications and Science (ATLAS) 3 mission (3–12 November 1994)¹⁵ with ATMOS filter 12 covering

Table 1. ATMOS/ATLAS 3 occultations analyzed in this study

Event	Date 1994 UT	Lat. deg N	Long. deg E	Minimum tangent altitude (km)	Sky conditions	Trop. height (km)
Filter 3 (1550–3420 cm ⁻¹)						
SS70	November 9	31.4	94.0	9	CS	14.9
SS73	November 9	30.5	26.5	5	CS	13.9
SS76	November 10	26.5	184.3	5	CS	17.2
SS79	November 10	24.7	117.0	7	LAC	16.1
SS85	November 10	22.0	342.2	11	LAC	16.0
SS88	November 10	19.9	275.0	13	LAC	16.3
SS91	November 11	18.0	207.7	16	HAC	16.8
SS94	November 11	15.9	140.4	8	LAC	16.6
SS97	November 11	14.0	73.1	18	HAC	16.6
SS100	November 11	11.3	343.5	< 7	LC	16.6
SS103	November 11	8.6	276.4	18	HAC	16.5
SS106	November 12	6.6	209.1	13	LAC	16.7
Filter 12 (625–1400 cm ⁻¹)						
SS71	November 9	31.1	71.6	< 5	CS	16.0
SS74	November 9	30.2	4.0	< 5	CS	13.6
SS80	November 10	23.9	94.6	15	HAC	15.7
SS83	November 10	22.7	27.2	3	CS	16.2
SS86	November 10	21.4	319.7	< 5	CS	16.2
SS89	November 11	19.1	252.6	16	HAC	16.4
SS92	November 11	17.8	185.1	17	HAC	16.8
SS95	November 11	15.2	118.0	6	LAC	16.6
SS98	November 11	13.0	50.8	12	HAC	16.4
SS104	November 12	8.0	253.9	< 5	LC	16.6
SS107	November 12	5.3	186.8	14	HAC	16.8

Latitude (Lat.) and longitude (Long.) at the tangent point for the spectrum nearest to a tangent altitude of 15 km. SS = sunset. Qualitative classification of upper tropospheric measurements: CS = clear sky; HAC = high altitude cirrus (maximum altitude >15 km); LAC = low altitude cirrus (maximum altitude <15 km); LC = layered cirrus. Tropopause (Trop.) heights are from NMC data.

625–1400 cm^{-1} at a signal to root-mean-square (rms) noise ratio of ~ 250 and filter 3 covering 1550–3420 cm^{-1} at a signal-to-rms-noise ratio of ~ 100 . Each low Sun spectrum was divided by an average exoatmospheric spectrum from the same occultation to remove instrumental and solar spectral features.

During the ATLAS 3 mission, ATMOS FTS observations were recorded during 107 sunsets with tangent point latitudes between 5°N and 49°N and 94 sunrises with tangent point latitudes between 64°S and 72°S .¹⁶ Tropical and subtropical measurements, the focus of this paper, were obtained late in the mission at relatively high beta angles. The spacing in refracted tangent height for successive tropical and subtropical observations (~ 1 km near the tropopause) was one half to one-third the typical ATMOS value. The effective vertical resolution of these observations was limited principally by the finite interferogram scan time and the circular instrumental field of view on the Sun: 1.0 mrad in diameter (2.0 km at the tangent point) for filter 3 observations and 2.0 mrad in diameter (4.0 km at the tangent point) for filter 12 observations. The range in tangent point latitude and longitude sampled during an occultation varied significantly near the end of the mission, but it did not exceed 2° between tangent heights of 15 and 30 km. Table 1 provides a list of the 23 tropical and subtropical occultations analyzed in this study. Papers by Norton and Rinsland¹⁷ and Abrams et al¹⁸ describe the ATMOS data processing and analysis methods used previously to retrieve stratospheric gas volume mixing ratio profiles from series of microwindows selected in the ATMOS spectra.

Table 2. Microwindows used to retrieve the profiles reported in this study

Spectral region (cm^{-1})	Tangent altitude range (km)	Interfering molecules*
<i>HCN</i>		
753.05–753.60	11.0–16.0	O_3
761.95–762.30	11.0–16.0	C_2H_2 , O_3
3271.29–3271.59	14.0–27.0	None
3274.46–3274.75	14.0–27.0	None
3277.70–3278.00	14.0–32.0	None
3280.87–3281.17	16.0–32.0	None
3287.06–3287.34	15.0–32.0	None
3299.42–3299.68	15.0–30.0	None
3302.40–3302.70	15.0–30.0	None
3305.34–3305.74	14.0–28.0	None
3334.15–3334.45	14.0–32.0	None
3337.00–3337.30	15.0–32.0	None
3342.55–3342.75	17.0–32.0	None
3358.37–3358.57	15.0–25.0	None
<i>CO</i>		
2135.19–2135.89	18.0–110.0	O_3
2138.93–2139.93	18.0–100.0	O_3
2140.50–2141.10	8.0–18.0	O_3
2146.68–2147.48	18.0–100.0	O_3 , N_2O
2153.30–2153.55	8.0–18.0	O_3
2157.80–2158.80	18.0–105.0	O_3 , N_2O
2179.57–2179.97	18.0–110.0	O_3 , N_2O
2183.00–2183.40	40.0–110.0	None
2186.24–2187.04	50.0–110.0	None
2189.50–2190.30	50.0–115.0	None
<i>C_2H_2</i>		
754.86–755.05	11.0–16.0	O_3
761.95–762.30	11.0–16.0	O_3 , HCN
766.60–766.95	11.0–16.0	O_3
776.04–776.15	11.0–16.0	None
<i>C_2H_6</i>		
2976.06–2977.14	8.0–16.0	CH_4 , O_3

* Includes only the interference by lines within the microwindow interval. In some cases, especially at low altitudes, the slope of the background in the microwindow is affected by wing absorption from distant, intense lines (usually H_2 ^{16}O transitions).

3. RETRIEVALS OF MOLECULAR VOLUME MIXING RATIO PROFILES

The volume mixing ratio profiles reported in this paper were retrieved with an algorithm that is based on the global-fit approach of Carlotti.¹⁹ It has been used previously to retrieve molecular profiles of H₂O, CH₄, and their isotopes from the ATMOS Spacelab 3 spectra.²⁰ In the global-fit approach, gas profiles are retrieved by simultaneously analyzing a series of spectra recorded during an occultation event. The advantages of the global-fitting technique relative to the onion-peeling technique have been discussed by Carlotti.¹⁹ In the present implementation, profiles of one or more gases are derived from simultaneous fittings of all measurements obtained in prespecified sets of microwindows and corresponding tangent altitude ranges. In this approach, regions with poorly determined or temperature-sensitive lines are avoided and interfering lines overlapping the target absorptions are fitted. The signal corresponding to the 100% transmittance level is determined for each microwindow. Hence, the retrieval method is insensitive to extinction by broad continua, such as extinction by clouds or aerosols.

Table 2 lists the microwindows selected for the analysis of the 4 target trace gases. The selection of these regions and retrievals reported here are based on the 1995 ATMOS compilation.²¹ Only features with intensities insensitive to temperature and free of overlapping interferences were analyzed. Except for CO, target features were fitted with line center absorption depths less than ~30%. It was necessary to relax this criterion for CO because of its strong absorption in the filter 3 upper tropospheric spectra.

The process of determining the viewing geometry and retrieving temperature as a function of pressure above the tropopause relied on spacecraft ephemeris information and a rotational analysis of retrieved apparent abundances from CO₂ temperature-independent and CO₂ temperature-dependent rovibrational absorption lines in microwindows.²² The CO₂ volume mixing ratio versus altitude profile²⁵ was assumed. Version 2 ATMOS results, which included a final pressure sounding to ensure that the measured slant-path CO₂ columns are consistent with the assumed volume mixing ratio profile,²³ were adopted in this work with minor updates. Correlative National Meteorological Center (NMC) pressure-temperature profiles²⁴ were used to extend the physical models into the upper troposphere. Tangent pressures were determined for the upper tropospheric spectra by fitting isolated CO₂ lines with temperature-insensitive intensities. The set of CO₂ microwindows used for stratospheric and mesospheric pressure sounding from ATMOS spectra²³ was augmented for the analysis.

Filter 12 observations present unique difficulties for the retrieval of accurate tangent pressures in the upper troposphere because of the limited number of unblended, temperature-insensitive CO₂ lines within the spectral range of the measurements. The only suitable lines are transitions of the ¹²C¹⁶O¹⁸O ν_1 band in the 1230–1250 cm⁻¹ region. To validate the tangent pressures derived from those lines, we retrieved profiles of N₂O from measurements of temperature-insensitive lines in the $2\nu_2$ band. The mixing ratio of N₂O varies widely in the stratosphere, but it is nearly uniform in the troposphere with relative fluctuations of 1% or less.²⁵ In 1994, the N₂O mixing ratio in the tropical troposphere was ~310 ppbv (1 ppbv=10⁻⁹ by volume).²⁶ The retrieved filter 12 N₂O mixing ratios derived below the NMC-determined tropopause are consistent with this value within the uncertainty of the retrievals (± 5 – $\pm 10\%$). Similarly, we used retrievals of N₂O and N₂ mixing ratios to check the retrieved tangent pressures for filter 3 spectra.

The total uncertainty due to random errors and the total uncertainty due to systematic errors have been derived by computing the square root of the sum of the squares of the contributions from the individual error components. Table 3 lists the error sources and the uncertainty values adopted in these calculations. The total errors have been computed by summing the total random and total systematic errors. Errors due to uncertainty in the spectroscopic parameters are largest for C₂H₆. Although the 1995 ATMOS compilation parameters²¹ for the target ^PQ₃ ν_7 band subbranch are more accurate than those on HITRAN 1996,²⁷ neither compilation includes the more accurate parameters reported recently for this feature.²⁸ Further analysis of the same set of laboratory C₂H₆ spectra to improve the parameters for the ^PQ₃ ν_7 band subbranch region is in progress.²⁹

Figure 1 shows portions of ATMOS filter 12 spectra recorded near a tangent pressure of 160 mbar (13.4 km altitude) during occultations SS98 and SS104. Arrows mark lines of the ν_2 band of HCN and the ν_5 band of C₂H₂. Both absorption features are significantly stronger in SS98 than in SS104. The other absorptions, lines of O₃ and CO₂, have similar depths in the two spectra. Although strong

Table 3. Error budget for species included in this study

Relative 1 σ error (%) in volume mixing ratio for an individual occultation						
Error source	Error type*	Molecule (filter number)				
		CO(3)	C ₂ H ₂ (12)	HCN(3)	HCN(12)	C ₂ H ₆ (3)
I. Observational geometry						
(a) Reference pressure	S	2	2	2	2	2
(b) Tangent pressure	R	4	8	4	8	4
(c) Temperature profile	R	1	1	1	1	1
II. Algorithm						
	S	<5	<5	<5	<5	<5
III. Observational data						
(a) Finite signal-to-noise	R	4	3	4	3	4
(b) Zero transmission offsets	R	3	1	1	1	1
	S	3	1	1	1	1
IV. Spectroscopic parameters						
	S	1	7	5	7	13
V. Interfering species						
	S	5	5	0	6	4
Total systematic error		4	9	5	9	15
Total random error		6	9	6	9	6

*S = systematic, R = random. The 5% upper limit for algorithm uncertainty is not included in calculating the total systematic error.

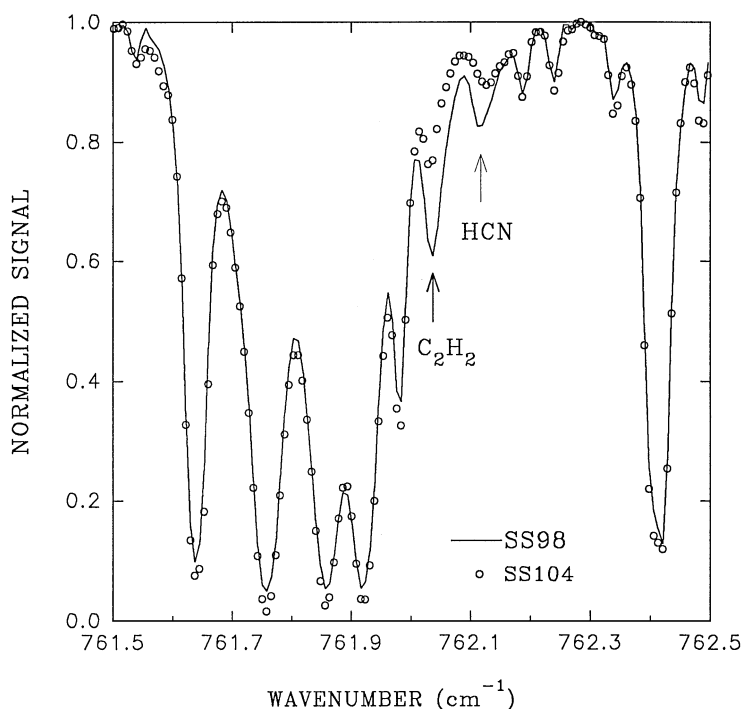


Fig. 1. ATMOS filter 12 spectra recorded near a tangent pressure of 160 mbar (13.4 km altitude) during occultations SS98 and SS104. Arrows mark the R13 line of the ν_5 band of C₂H₂ at 762.0400 cm⁻¹ and the R16 line of the ν_2 band of HCN at 762.1206 cm⁻¹.

absorptions by O₃ and CO₂ mask many of the HCN and C₂H₂ lines in the 13 μ m region, the available target features (Table 2) are consistent in showing large enhancements in both gases near 160 mbar during occultation SS98. This occultation was recorded over the mouth of the gulf of Aden, at the easternmost tip of Africa.

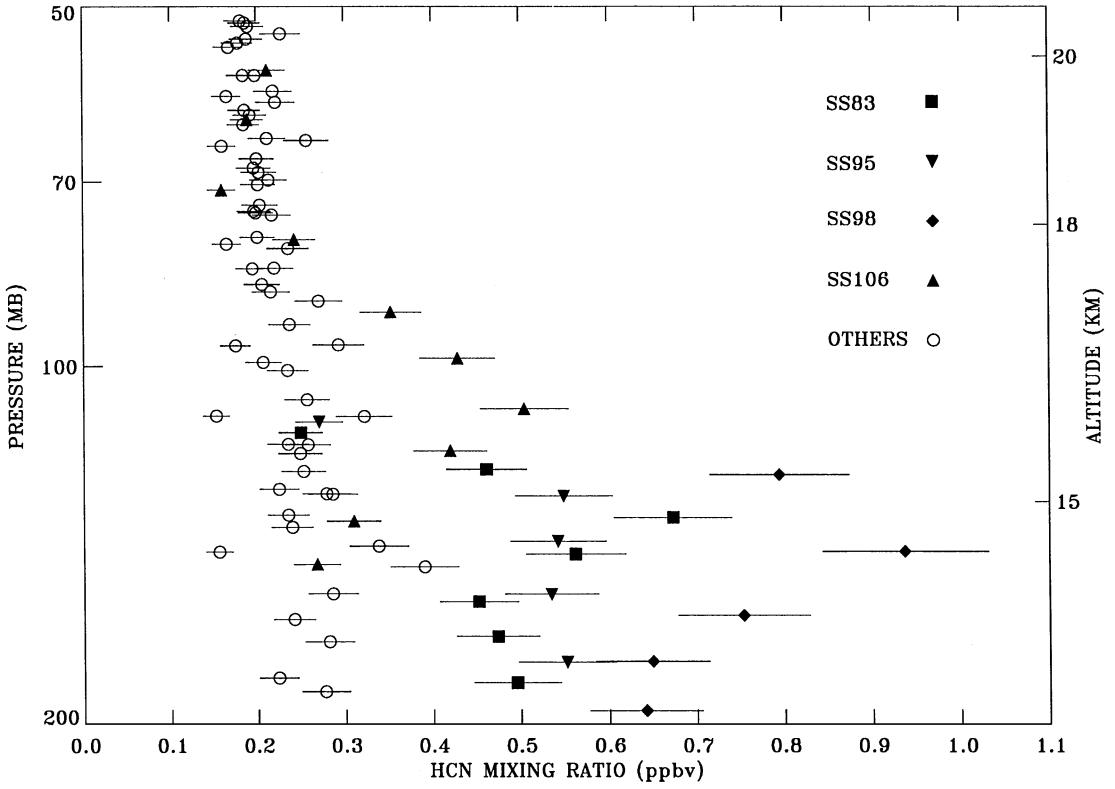


Fig. 2.

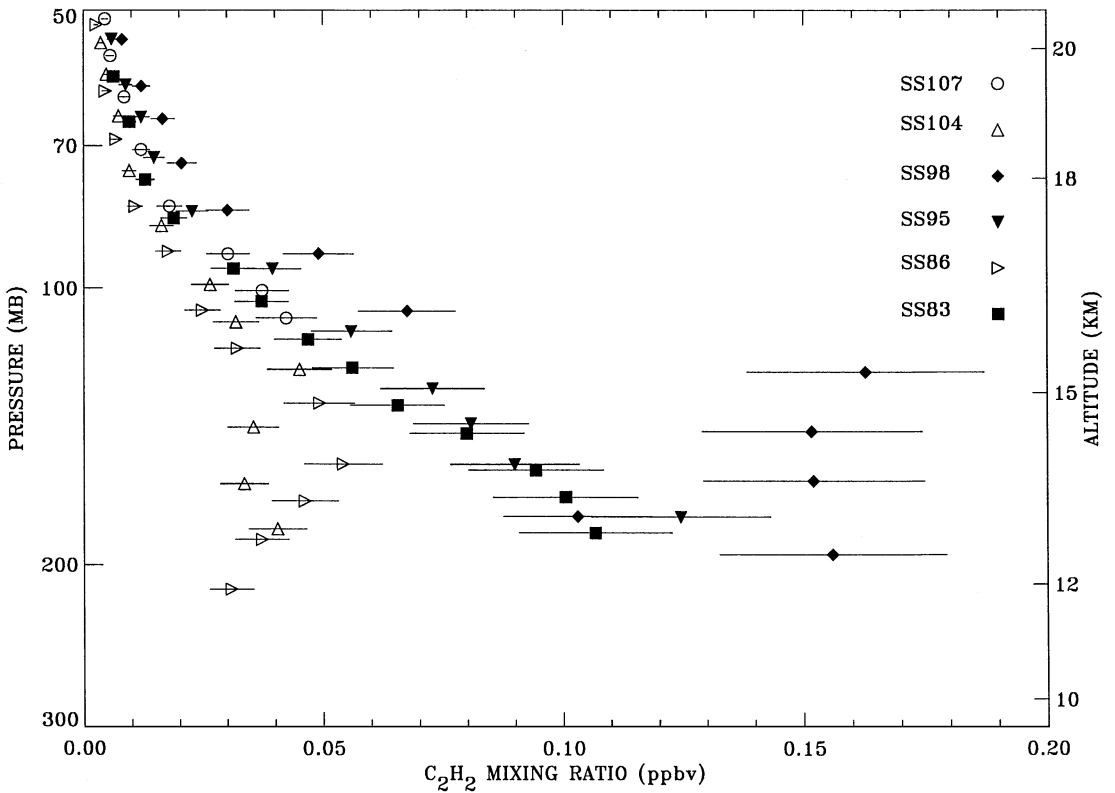


Fig. 3.

Figure 2 shows the profiles of HCN retrieved from the filter 3 and 12 tropical spectra. The stratospheric measurements are near a mixing ratio of ~ 0.2 ppbv, consistent with both 1985 ATMOS Spacelab 3 and the November 1994 ATMOS/ATLAS 3 30°N latitude stratospheric profile measurements,³⁰ 28°N and 48°S latitude upper tropospheric profiles derived down to ~ 150 mbar from the ATMOS Spacelab 3 spectra,³¹ and most of the IR total column measurements obtained from Kitt Peak at 31.9°N and the Jungfraujoch at 46.5°N latitude.³² However, about half of the occultations show elevated HCN at lower altitudes with a maximum mixing ratio of 0.94 ± 0.19 ppbv at 140 mbar measured from SS98. The Kitt Peak and Jungfraujoch ground-based studies³² found evidence for variable enhancements in HCN mixing ratios during spring with total column increases by up to factors of 3 and 2, respectively. While these observations represent evidence for occasional, large enhancements in tropospheric HCN, they were obtained from northern midlatitude stations, with the springtime enhancements attributed to the tropospheric layers above the stations on the basis of the broader measured lines. Therefore, these enhancements may involve emission processes unrelated to those responsible for the high mixing ratios we have detected in the tropical upper troposphere.

To our knowledge, no other remote sensing measurements of HCN in the upper troposphere have been reported. However, the possible importance of HCN in the tropics has been noted recently on the basis of aircraft *in situ* measurements obtained during the GTE/TRACE A mission.^{5,6} Total reactive nitrogen (NO_y) derived by summing measurements of individual components, principally PAN, NO, NO_2 , and HNO_3 , was found to be slightly less than half the value determined from simultaneous measurements with an instrument designed to convert and measure the NO_y sum. Above 8 km, the production of NO_x ($\text{NO} + \text{NO}_2$) balances on average only 16% of the loss.³³ On the basis of the GTE/TRACE A measurements and measured fire emission factors,³⁴ Singh et al⁶ and Smyth et al⁵ suggested that a substantial fraction of the “missing” NO_y may be due to HCN with expected mixing ratios of 0.3 to >2 ppbv in high-altitude plumes.⁵ Tropical fires may be the dominant source of atmospheric HCN.³⁴ In organic soil, where the HCN/ NH_3 emission ratio varies by two orders of magnitude, HCN is sometimes the dominant, detected nitrogen-containing product of smoldering combustion.³⁵ Although it has also been suggested that HCN may serve as a global tracer of biomass burning emissions,³⁴ total HCN emissions make up only several percent of the fuel nitrogen during open fires.^{36–38} The frequent occurrence of elevated upper tropospheric HCN mixing ratios in the ATMOS/ATLAS 3 tropical dataset suggests the need for additional laboratory fire and field measurements of tropical HCN.

Figure 3 presents the profiles of C_2H_2 retrieved from the filter 12 tropical observations. As already mentioned, occultation SS98 shows elevated C_2H_2 mixing ratios in the upper troposphere; the C_2H_2 layer of ~ 0.15 ppbv at 120–160 mbar shows the maximum observed enhancements. Elevated C_2H_2 and HCN mixing ratios (solid symbols in both Figs. 2 and 3) also occur for several other occultations. To our knowledge, no correlative measurements of C_2H_2 are available for comparison. However, the elevated C_2H_2 values are similar to the mixing ratios measured in high altitude air parcels originating in continental outflow regions of the tropical south Atlantic during the TRACE A mission.⁸

Both CO and C_2H_6 have tropical photochemical lifetimes of about one month⁷ and similar combustion-related sources at the surface (except methane oxidation is not a source of C_2H_6). On this basis, significant enhancements of CO and C_2H_6 originating from fresh emissions are expected to be correlated, as has been observed over Brazil and southern Africa during the TRACE-A mission.⁷ Figure 4 illustrates tropical filter 3 spectra showing the variability of C_2H_6 absorption observed by ATMOS from spectra with similar tangent pressures in the upper troposphere.

Figures 2 and 3 on opposite page

Fig. 2. Upper tropospheric and lower stratospheric profiles of HCN retrieved from the ATMOS filter 3 and 12 tropical and subtropical spectra plotted versus pressure. Error bars show estimated 1 sigma total uncertainties. Solid symbols are used to identify measurements from occultations with elevated HCN mixing ratios in the upper troposphere. Measurements from other occultations (see Table 1) are shown with open circles.

Fig. 3. Upper tropospheric profiles of C_2H_2 retrieved from the ATMOS filter 12 tropical and subtropical spectra plotted versus pressure. Error bars show estimated $1 - \sigma$ total uncertainties. The solid symbols are the same as in Fig. 2; they have been used to highlight measurements with elevated mixing ratios.

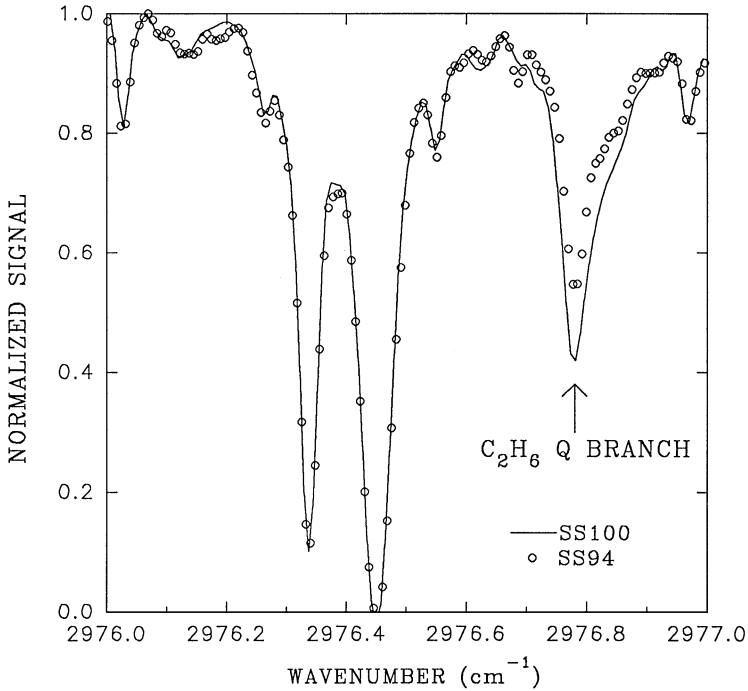


Fig. 4. ATMOS filter 3 spectra recorded near a tangent pressure of 135 mbar (14.8 km altitude) during occultations SS94 and SS100. An arrow marks the unresolved pQ_3 subbranch of the ν_7 band of C_2H_6 at 2976.8 cm^{-1} .

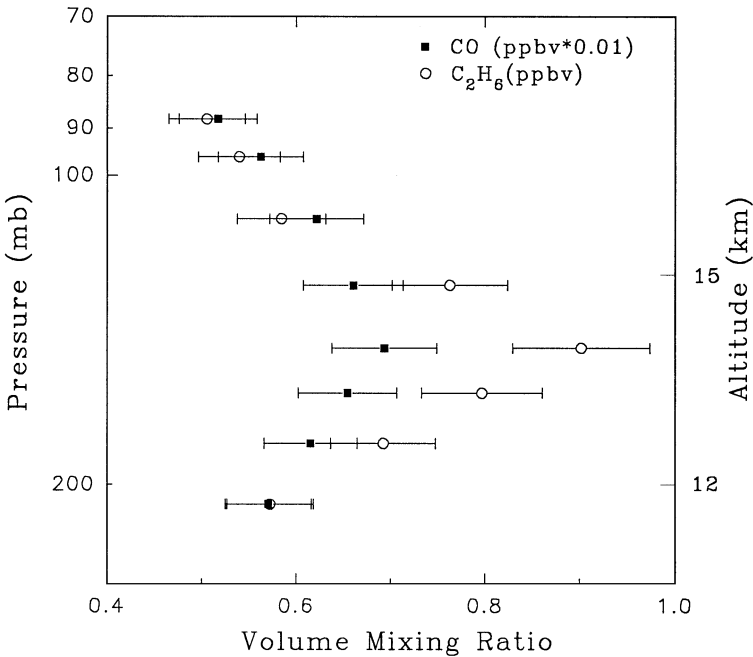


Fig. 5. Upper tropospheric profiles of C_2H_6 and CO retrieved from occultation SS100 plotted versus pressure. Error bars show estimated 1 sigma total uncertainties.

Correlated variations in CO and C_2H_6 have been detected. In Fig. 5 we present a plot of the mixing ratios of both gases measured between 88 and 209 mbar (12–17 km altitude) from occultation SS100, recorded over the westernmost point of Africa. The highest upper tropospheric C_2H_6 and CO mixing ratios were measured from this occultation. The vertical distributions of both gases show

peak mixing ratios near 150 mbar with an average ratio of 10.8 ± 1.3 pptv C_2H_6 /ppbv CO over the measured altitude range ($1 \text{ pptv} = 10^{-12}$ by volume). This value is similar to the ratio of 12.1 derived by Talbot et al⁸ over the south Atlantic basin during September–October 1992. Blake et al⁷ derived C_2H_6 /CO emission ratios of 8.3 ± 0.3 and 5.2 ± 0.2 pptv/ppbv from measurements of biomass burning emissions in Brazil and Africa, respectively, and a value of 6.0 pptv C_2H_6 /ppbv CO was reported from measurements directly over active fires in Brazil and Zambia.²¹ On the basis of their measurements, Talbot et al⁸ concluded that sources besides biomass burning emissions contribute to the significant C_2H_6 enhancements they observed over the South Atlantic basin.

4. SUMMARY AND CONCLUSIONS

In this paper, we have reported profiles of four long-lived trace gases derived from an initial study of the 0.01 cm^{-1} resolution, broadband IR solar occultation spectra recorded in the tropical and northern hemisphere subtropical upper troposphere in November 1994. Enhanced mixing ratios of HCN, C_2H_2 , CO, and C_2H_6 of up to one order of magnitude relative to unperturbed profiles have been measured. The enhancements in these species are correlated and likely the result of deep convective transport of near surface emissions to the upper troposphere. The observed elevated mixing ratios of HCN may account for at least part of the “missing NO_y ” that was prevalent in the September–October 1992 tropical upper troposphere.

Although we have not attempted to associate the enhanced upper tropospheric mixing ratios with specific surface emissions of pollution and subsequent convective events, we note that the ATMOS observations were obtained at the end of the dry seasons in Africa and South America, and hence, it is quite likely that biomass burning emissions of these long-lived gases played a key role in the measured upper tropospheric mixing ratio enhancements.

Acknowledgements—Research at the Jet Propulsion Laboratory (JPL) was performed under contract to the National Aeronautics and Space Administration (NASA). Research at the University of Denver is supported by NASA and the National Science Foundation (NSF). Research at the University of Alabama was supported by NASA’s Atmospheric Chemistry Modeling and Analysis Program. Research at Science and Technology Corporation (STC) and Science Applications International Corporation (SAIC) is also supported by NASA. The University of Liège involvement in the ATMOS project was partly supported by the Belgian “Global Change” program coordinated by the O.S.T.C., Brussels. We thank Linda Chiou of SAIC for her help in the analysis of the ATMOS spectra and the preparation of the figures. We are also grateful to Jack Fishman of NASA Langley, Geoff Toon of JPL, and Barney Farmer for helpful discussions during the development of this manuscript, and we acknowledge with thanks the comments from two anonymous referees.

REFERENCES

1. Danielsen, E. F., *In situ* evidence of rapid, vertical, irreversible transport of lower tropospheric air into the lower tropical stratosphere by convective cloud turrets and by large-scale upwelling in tropical cyclones, *J. Geophys. Res.*, 1993, **98**, 8665–8681.
2. Chatfield, R. B. and Crutzen, P. J., Sulfur dioxide in remote oceanic air: Cloud transport of reactive precursors, *J. Geophys. Res.*, 1984, **89**, 7111–7132.
3. Wang, C., Crutzen, P. J., Ramanathan, V. and Williams, S. F., The role of a deep convective storm over the tropical Pacific ocean in the redistribution of atmospheric chemical species, *J. Geophys. Res.*, 1995, **100**, 11 509–11 516.
4. Pickering, K. E., Thompson, A. M., Wang, Y., Tao, W.-K., McNamara, D. P., Kirchoff, V. W. J. H., Heikes, B. G., Sachse, G. W., Bradshaw, J. D., Gregory, G. L. and Blake, D. R., Convective transport of biomass burning emissions over Brazil during TRACE A, *J. Geophys. Res.*, 1996, **101**, 23 993–24 012.
5. Smyth, S. B., Sandholm, S. T., Bradshaw, J. D., Talbot, R. W., Blake, D. R., Blake, N. J., Rowland, F. S., Singh, H. B., Gregory, G. L., Anderson, B. E., Sachse, G. W., Collins, J. E. and Bachmeier, A. S., Factors influencing the upper free tropospheric distribution of reactive nitrogen over the south Atlantic during the TRACE A experiment, *J. Geophys. Res.*, 1996, **101**, 24 165–24 186.
6. Singh, H. B., Herlth, D., Koyler, R., Chatfield, R., Viezee, W., Salas, L. J., Chen, J., Bradshaw, J. D., Sandholm, S. T., Talbot, R., Gregory, G. L., Anderson, B., Sachse, G. W., Browell, E., Bachmeier, A. S., Blake, D. R., Heikes, B., Jacob, D. and Fuelberg, H. E., Impact of biomass burning emissions on the composition of the south Atlantic troposphere: Reactive nitrogen and ozone, *J. Geophys. Res.*, 1996, **101**, 24 203–24 219.
7. Blake, N. J., Blake, D. R., Sive, B. C., Chen, T.-Y., Rowland, F. S., Collins Jr. J. E., Sachse, G. W. and Anderson, B. E., Biomass burning emissions and vertical distribution of atmospheric methyl halides and other reduced carbon gases in the south Atlantic region, *J. Geophys. Res.*, 1996, **101**, 24 151–24 164.

8. Talbot, R. W., Bradshaw, R. D., Sandholm, S. T., Smyth, S., Blake, D. R., Blake, N. R., Sachse, G. W., Collins, J. E., Heikes, B. G., Anderson, B. E., Gregory, G. L., Singh, H. B., Lefer, B. L. and Bachmeier, A. S., Chemical characteristics of continental outflow over the tropical south atlantic ocean from Brazil and Africa, *J. Geophys. Res.*, 1996, **101**, 24 187–24 202.
9. Pickering, K. E., Thompson, A. M., Scala, J. R., Tao, W.-K., and Simpson, J., Ozone production potential following convective redistribution of biomass burning emissions, *J. Atmos. Chem.*, 1992, **14**, 297–313.
10. Browell, E. V., Fenn, M. A., Butler, C. F., Grant, W. B., Clayton, M. B., Fishman, J., Bachmeier, A. S., Anderson, B. E., Gregory, G. L., Fuelberg, H. E., Bradshaw, J. D., Sandholm, S. T., Blake, D. R., Heikes, B. G., Sachse, G. W., Singh, H. B. and Talbot, R. W., Ozone and aerosol distributions and air mass characteristics over the south atlantic basin during the burning season, *J. Geophys. Res.*, 1996, **101**, 24043–24068.
11. McKeen, S. A., Liu, S. C., Hsie, E.-Y., Lin, X., Bradshaw, J. D., Smyth, S., Gregory, G. L. and Blake, D. R., Hydrocarbon ratios during PEM-WEST A: A model perspective, *J. Geophys. Res.*, 1996, **101**, 2087–2109.
12. Rinsland, C. P., Gunson, M. R., Wang, P.-H., Arduini, R. F., Baum, B. A., Minnis, P., Goldman, A., Abrams, M. C., Zander, R., Mahieu, E., Salawitch, R. J., Michelsen, H. A., Irion, F. W. and Newchurch, M. J., ATMOS/ATLAS 3 infrared profile measurements of clouds in the tropical and subtropical upper troposphere, *JQSRT*, 1998, this issue.
13. Farmer, C. B., High resolution infrared spectroscopy of the sun and earth's atmosphere from space, *Mikrochim. Acta [Wien]*, 1987, **III**, 189–214.
14. Farmer, C. B., Raper, O. F. and O'Callaghan, F. G., Final report on the first flight of the ATMOS instrument during the Spacelab 3 mission, April 29–May 6, 1985, *JPL Publ.* 87-32, 45pp., Jet Propulsion Laboratory, Pasadena, California, 1 October 1987.
15. Kaye, J. A. and Miller, T. L., The ATLAS series of shuttle missions, *Geophys. Res. Lett.*, 1996, **23**, 2285–2288.
16. Gunson, M. R., Abbas, M. M., Abrams, M. C., Allen, M., Brown, L. R., Brown, T. L., Chang, A. J., Goldman, A., Irion, F. W., Lowes, L. L., Mahieu, E., Manney, G. L., Michelsen, H. A., Newchurch, M. J., Rinsland, C. P., Salawitch, R. J., Stiller, G. P., Toon, G. C., Yung, Y. L. and Zander, R., The atmospheric trace molecule spectroscopy (ATMOS) experiment: Deployment on the ATLAS space shuttle missions, *Geophys. Res. Lett.*, 1996, **23**, 2333–2336.
17. Norton, R. H. and Rinsland, C. P., ATMOS data processing and science analysis methods, *Appl. Opt.*, 1991, **30**, 389–400.
18. Abrams, M. C., Chang, A. Y., Gunson, M. R., Abbas, M. M., Goldman, A., Irion, F. W., Michelsen, H. A., Newchurch, M. J., Rinsland, C. P., Stiller, G. P. and Zander, R., On the assessment and uncertainty of atmospheric trace gas burden measurements with high resolution infrared solar occultation spectra from space by the ATMOS experiment, *Geophys. Res. Lett.*, 1996, **23**, 2337–2340.
19. Carlotti, M., Global-fit approach to the analysis of limb-scanning atmospheric measurements, *Appl. Opt.*, 1988, **27**, 3250–3254.
20. Rinsland, C. P., Gunson, M. R., Foster, J. C., Toth, R. A., Farmer, C. B. and Zander, R., Stratospheric profiles of heavy water vapor isotopes and CH₃D from analysis of the ATMOS spacelab 3 infrared solar spectra, *J. Geophys. Res.*, 1991, **96**, 1057–1068.
21. Brown, L. R., Gunson, M. R., Toth, R. A., Irion, F. W., Rinsland, C. P., and Goldman, A., 1995 atmospheric trace molecule spectroscopy (ATMOS) linelist, *Appl. Opt.*, 1996, **35**, 2828–2848.
22. Stiller, G. P., Gunson, M. R., Lowes, L. L., Abrams, M. C., Raper, O. F., Farmer, C. B., Zander, R. and Rinsland, C. P., Stratospheric and mesospheric pressure–temperature profiles from the rotational analysis of CO₂ lines in ATMOS/ATLAS-1 infrared solar occultation spectra, *J. Geophys. Res.*, 1995, **100**, 3107–3117.
23. Abrams, M. C., Gunson, M. R., Lowes, L. L., Rinsland, C. P. and Zander, R., Pressure sounding of the middle atmosphere from ATMOS solar occultation measurements of atmospheric CO₂ absorption lines, *Appl. Opt.*, 1996, **35**, 2810–2820.
24. Gelman, M., National Meteorological Center, private communication, 1994.
25. Warneck, P., *Chemistry of the Natural Atmosphere*, Chap. 9, Academic, San Diego, 1988.
26. Hofmann, D. J. and Peterson, J. T. eds., *Climate Monitoring and Diagnostics Laboratory No. 23 Summary Report 1994–1995*, U. S. Department of Commerce, National Oceanic and Atmospheric Administration, Environmental Research Laboratories, Chap. 5, National Technical Information Service, 5285 Port Royal Road, Springfield, VA, 1996.
27. Rothman, L. S., Rinsland, C. P., Goldman, A., Massie, S. T., Edwards, D. P., Flaud, J.-M., Perrin, A., Dana, V., Mandin, J.-Y., Schroeder, J., McCann, A., Gamache, R. R., Wattson, R. B., Yoshino, K., Chance, K., Jucks, K., Brown, L. R., Nemtchinov, V. and Varanasi, P., The HITRAN molecular spectroscopic database and HAWKS (HITRAN atmospheric workstation): 1996 edn, *JQSRT*, 1998, this issue.
28. Pine, A. S. and Stone, S. C., Torsional tunneling and A₁–A₂ splittings and air broadening of the ^νQ₀ and ^νQ₃ subbranches of the ν₇ band of ethane, *J. Mol. Spectrosc.*, 1996, **175**, 21–30.
29. Pine, A. S., private communication, 1997.
30. Rinsland, C. P., Mahieu, E., Zander, R., Gunson, M. R., Salawitch, R. J., Chang, A. Y., Goldman, A., Abrams, M. C., Abbas, M. M., Newchurch, M. J. and Irion, F. W., Trends of OCS, HCN, SF₆, CHClF₂ (HCFC-22) in the lower stratosphere from 1985 and 1994 atmospheric trace molecule spectroscopy experiment measurements near 30°N latitude, *Geophys. Res. Lett.*, 1996, **23**, 2349–2352.

31. Zander, R., Rinsland, C. P., Farmer, C. B., Namkung, J., Norton, R. H. and Russell III, J. M., Concentrations of carbonyl sulfide and hydrogen cyanide in the free upper troposphere and lower stratosphere deduced from ATMOS/Spacelab 3 infrared solar occultation spectra, *J. Geophys. Res.*, 1988, **93**, 1669–1678.
32. Mahieu, E., Rinsland, C. P., Zander, R., Demoulin, P., Delbouille, L. and Roland, G., Vertical column abundances of HCN deduced from ground-based infrared solar spectra, *J. Atmos. Chem.*, 1995, **20**, 299–310.
33. Jacob, D. J., Heikes, B. G., Fan, S.-M., Logan, J. A., Mauzerall, D. L., Bradshaw, J. D., Singh, H. B., Gregory, G. L., Talbot, R. W., Blake, D. R. and Sachse, G. W., Origin of ozone and NO_x in the tropical troposphere: A photochemical analysis of aircraft observations over the south atlantic basin, *J. Geophys. Res.*, 1996, **101**, 24 235–24 250.
34. Lobert, J. M., Scharffe, D. H., Hao, W. M. and Crutzen, P. J., Importance of biomass burning in the atmospheric budgets of nitrogen-containing gases, *Nature*, 1990, **346**, 552–554.
35. Yokelson, R. J., Susott, R., Ward, D. E., Reardon, J. and Griffith, D. W. T., Emissions from smoldering combustion of biomass measured by open-path FTIR, *J. Geophys. Res.*, 1998, **102**, 18 865–18 878.
36. Hurst, D. F., Griffith, D. W. T., Carras, J. N., Williams, D. J. and Fraser, P. J., Measurements of trace gases emitted by australian savanna fires during the 1990 dry season, *J. Atmos. Chem.*, 1994, **18**, 33–56.
37. Hurst, D. F., Griffith, D. W. T. and Cook, G. D., Trace gas emissions from biomass burning in tropical australian savannas, *J. Geophys. Res.*, 1994, **99**, 16 441–16 456.
38. Yokelson, R. J., Griffith, D. W. T. and Ward, D. E., Open-path Fourier transform infrared studies of large-scale laboratory biomass fires, *J. Geophys. Res.*, 1996, **101**, 21 067–21 080.